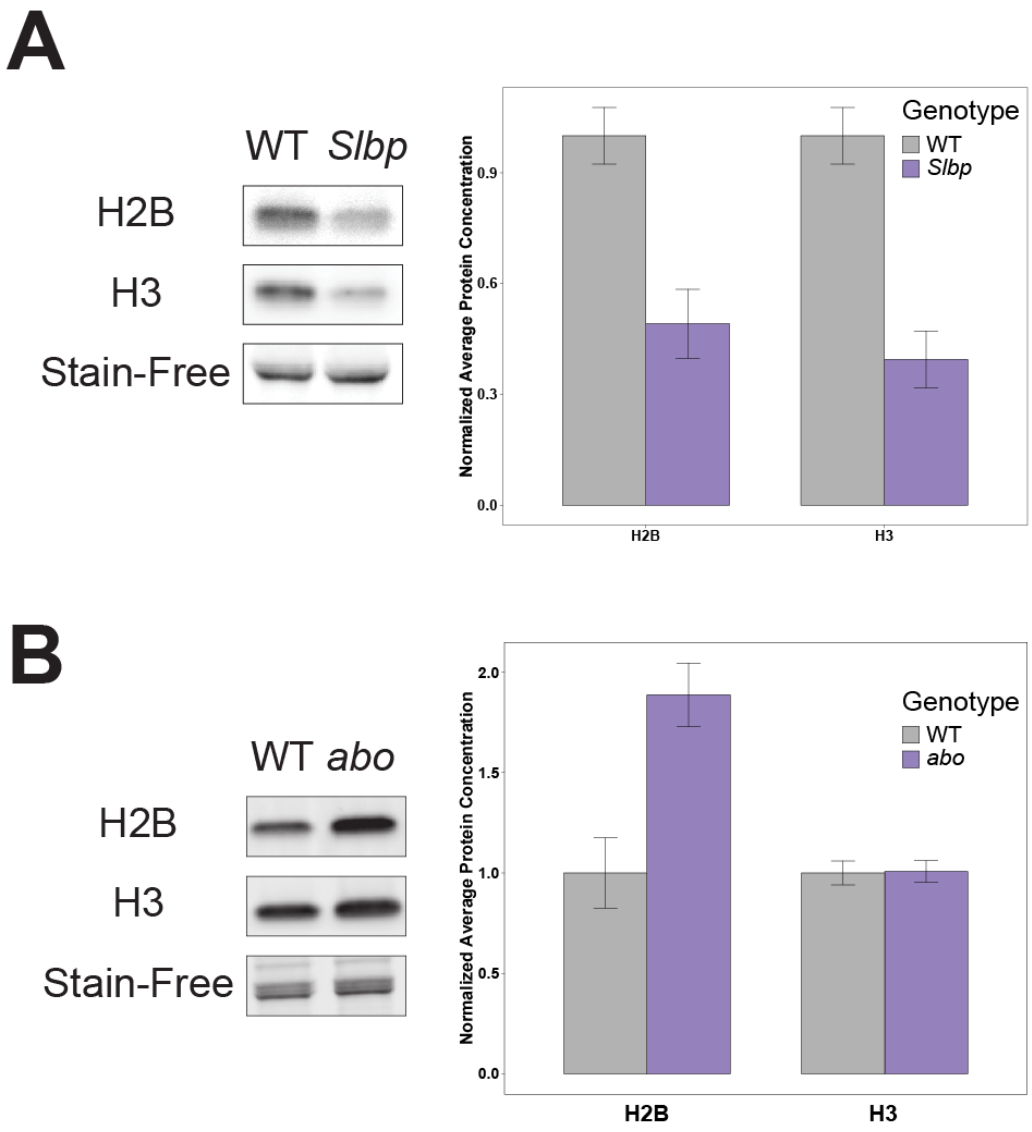

Figure S1. *Slbp* RNAi and *abo* embryos have altered histone protein levels
(A) Total H2B and H3 protein from WT and *Slbp* embryos collected 55 minutes after pole cell formation (early NC14 in WT) from western blotting with 5 embryos per lane. *Slbp* embryos have approximately a ~50% reduction in H2B protein and ~60% reduction in H3 protein (n=3). Bars represent mean and SEM. (B) Total H2B and H3 protein from *abo* embryos at collected 55 minutes after pole cell formation (early NC14 in WT) from western blotting. *abo* embryos have ~90% increase in H2B while total H3 was unchanged between WT (n=5) and *abo* (n=6) embryos. Bars represent mean and SEM. We note that the antibodies used for the assay cannot distinguish between the replication-coupled and replication-independent H3 variants and so the effect size on the replication-coupled H3 may be greater than reported here if there is compensation by the replication-independent variant.

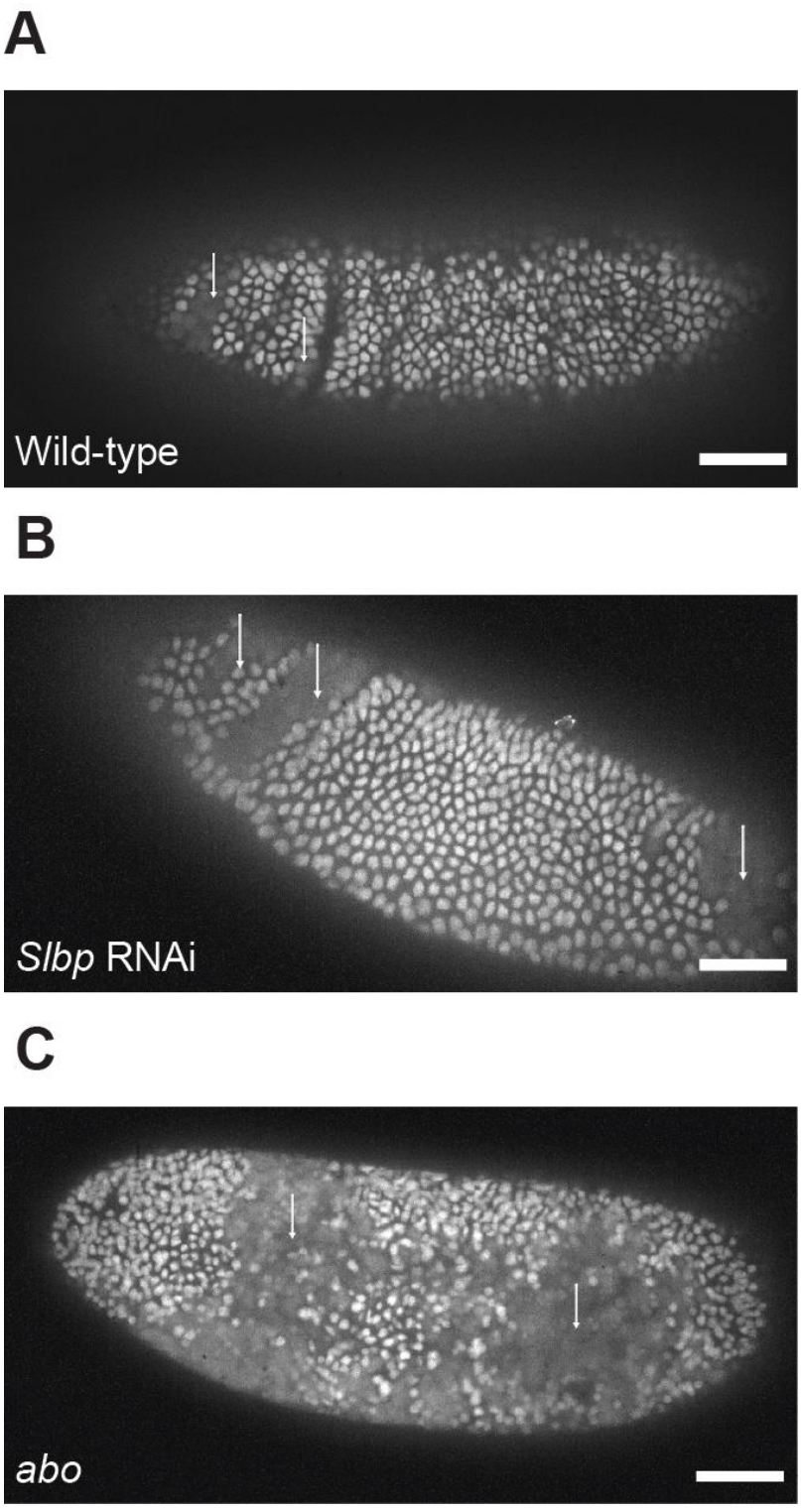

Figure S2. *Slbp* RNAi and *abo* embryos attempt post-MBT development
(A) WT embryo post-MBT after NC14. Mitotic domains and gastrulation movements form normally and with characteristic temporal and spatial dynamics. Arrows indicate mitotic domains. (B) *Slbp* embryo that enters gastrulation in NC13. Mitotic domain formation and gastrulation appear unaffected despite embryos having reduced numbers of cells. These embryos proceed through early-to-mid embryogenesis relatively normally but die before hatching. Arrows indicate mitotic domain formation. (C) *abo* embryos that enters gastrulation in NC15. *abo* embryos that undergo extra divisions still attempt post-MBT behaviors such as mitotic domain formation and gastrulation but are severely disrupted. Arrows indicate aberrant mitotic domain formation. Scale bar represents 50 μm.

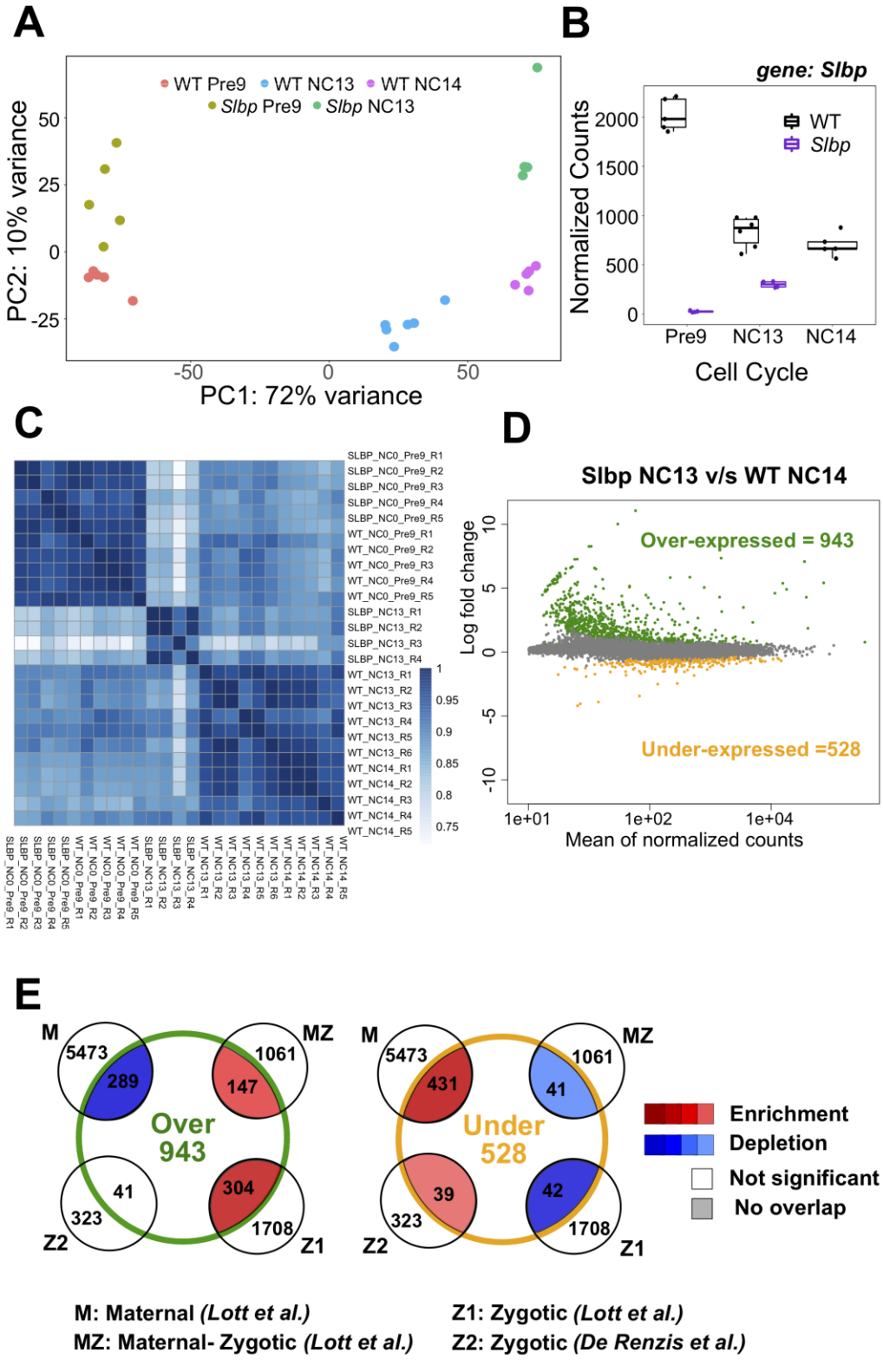

Figure S3. Depletion of maternal histones advance MZT
(A) Principal Components Analysis of *Slbp* and WT expression data demonstrating that global transcriptomic profile is shifted in *Slbp* NC13 as compared WT NC13 and is more similar to WT NC14 indicating that the onset of transcription is advanced in *Slbp* embryos. (B) Normalized counts of *Slbp* mRNA showing a reduction in *Slbp* mutants (n=5 in Pre9 and n=4 in NC13) as compared to WT (n=5 in Pre9, n=6 in NC13 and n=5 in NC14) (C) Spearman's correlation of expression data for WT and *Slbp* embryos at different timepoints. Replicates are more similar to each other than they are to other genotypes and timepoints. (D) When compared to time matched controls (NC14 +20') fewer genes are altered in expression. 943 genes are overexpressed and 528 genes are underexpressed, consistent with premature MZT in the *Slbp* embryos. (E) Data from C compared to previous datasets. Genes overexpressed compared to WT NC14 embryos show enrichment for zygotic transcripts while the underexpressed genes are enriched for maternal transcripts and show a slight enrichment for the De Renzis maternal genes.

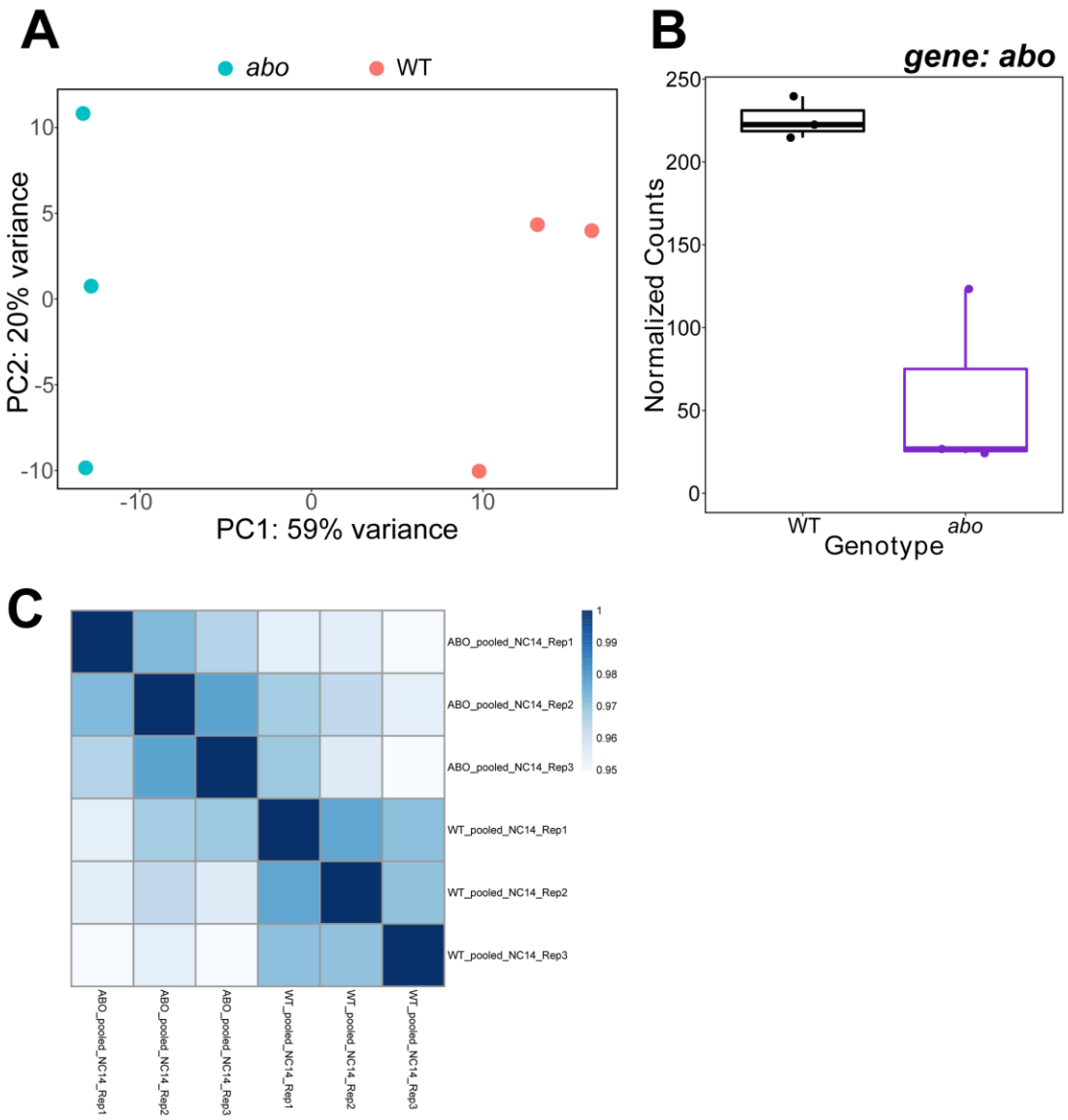

Figure S4. Global transcriptomic differences upon histone overexpression
(A) Principal Components Analysis between the pooled NC14 *abo* and WT expression data showing a clear difference in gene expression between genotypes at this developmental stage. (B) Normalized counts of *abo* mRNA showing reduction in *abo* mutants (n=3) as compared to WT (n=3). (C) Spearman's correlation of expression data for WT and *abo* embryos in NC14.

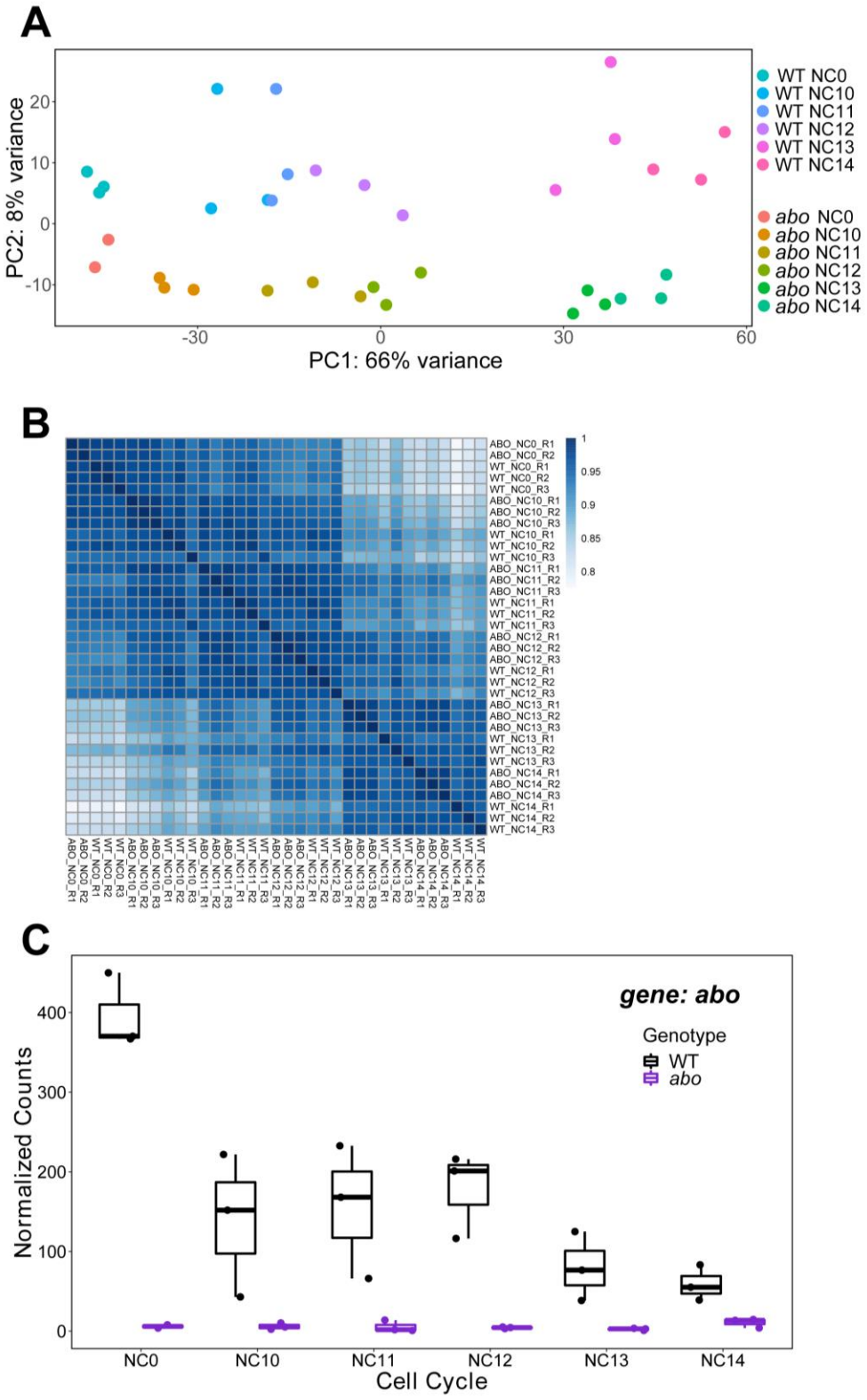

Figure S5. Timecourse transcriptomic differences upon histone overexpression
(A) Principal Components Analysis shows a clear separation across both cell cycle and genotype for the *abo* time-course experiment. (B)Spearman's correlation of expression data for WT and *abo* embryos across all timepoints. (C) Normalized counts of *abo* mRNA showing a reduction in *abo* mutants (n=2 at NC0 and n=3, all other time-points) as compared to WT (n=3, all time-points)

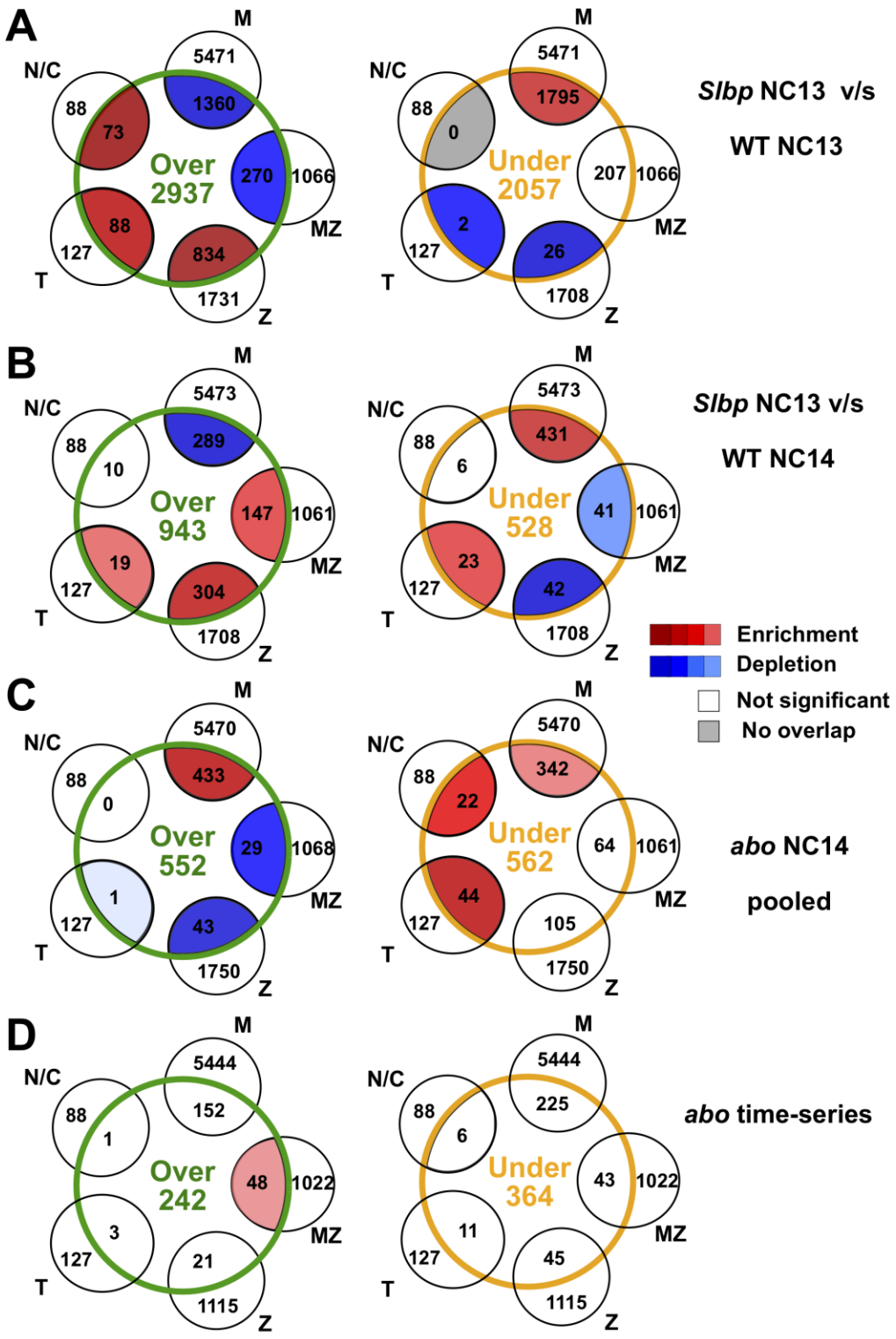

Figure S6. Histone sensitivity changes the onset of ZGA, but cannot explain previous N/C ratio dependent gene sets (A) *Slbp* NC13 compared to WT NC13. Data the same as Figure 2D except the De Renzis et al. (2007) maternal data has been split into N/C and time dependent genes as per Lu et al. (2009). Both N/C and time dependent genes are enriched in the overexpressed and depleted in the underexpressed categories, consistent with global advancement of the MZT. (B) *Slbp* NC13 compared to WT NC14. Data corresponds to Figure S3E. When controlled for time, enrichment of N/C ratio dependent genes is lost and time-dependent genes become enriched in both the over and under expressed gene sets. (C) *abo* NC14 compared to WT NC14. Data corresponds to Figure 3D. Both N/C and time dependent genes are enriched in the underexpressed category consistent with a global delay of ZGA. (D) *abo* time series comparison. Although not statistically significant, both N/C ratio and time dependent genes show an odds ratio >1 indicating these are also trending towards enrichment in the underexpressed gene set. Indeed, when the abo timecourse underexpressed genes are compared to De Renzis et. al (2007) zygotic genes dataset from which the N/C and time gene sets are derived the total zygotic overlap shows significant enrichment (p=9.9e-4) indicating that zygotic genes are better represented in the timecourse abo underexpressed group than the overexpressed set (Table S6).

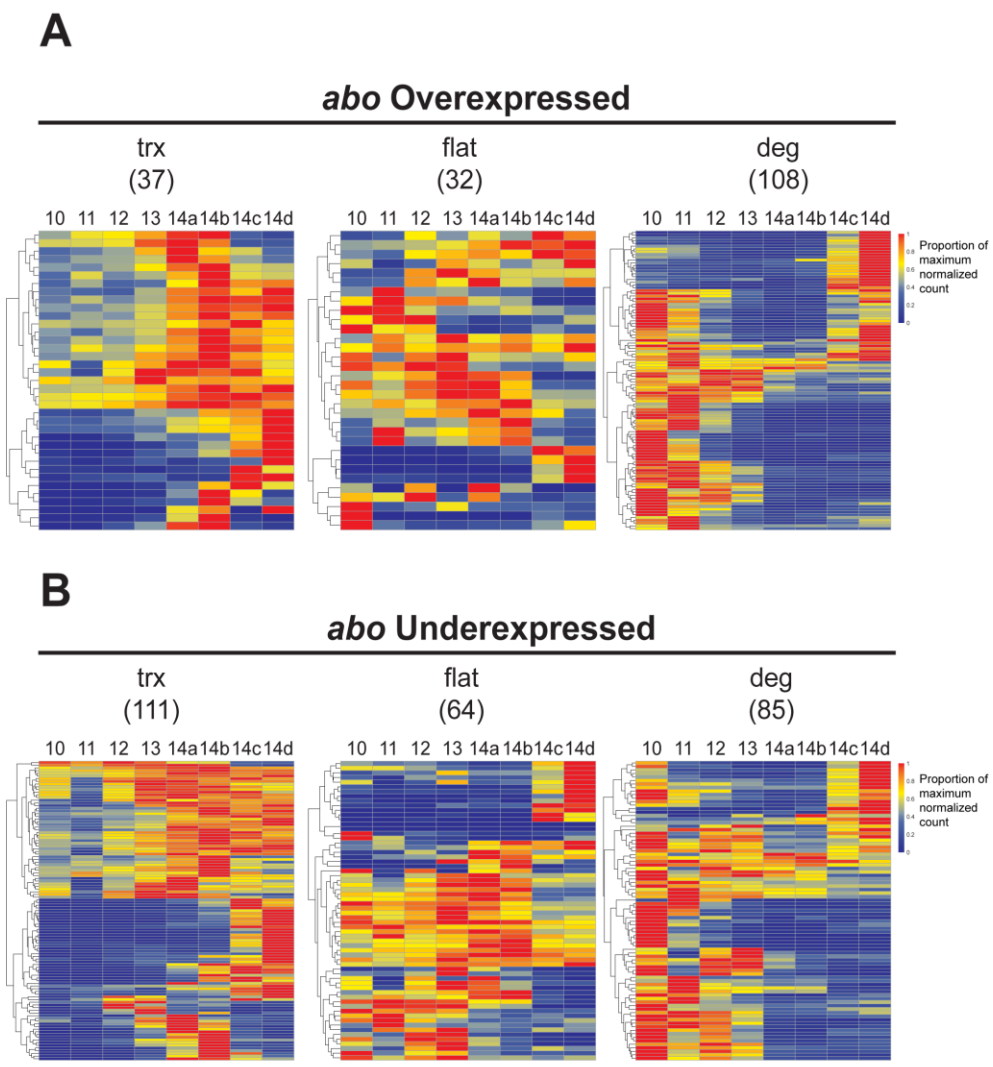

Figure S7. Genes that are knocked down by histone overexpression are expressed during WT MZT

(A) Overexpressed genes in the *abo* time series compared to longer time course from Lott et al. (2011). Each heatmap represents genes categorized as increasing (trx), remaining constant (flat), or decreasing (deg) from our control experiments (as in Figure 4). Numbers in parentheses indicate number of genes within the specified category. The majority of overexpressed genes are constant or downward trending, consistent with a delay in degradation of maternal products in histone overexpressing embryos. (B) *abo* underexpressed genes compared to Lott et al. (2011) Many of the underexpressed genes increase over time in WT supporting the idea there is a delay in zygotic transcription in *abo* embryos. Each of the heatmaps were generated by obtaining the median normalized count per gene per nuclear cycle and dividing these values by the maximum median normalized count value for that gene across all nuclear cycles. Thus, each of the cells in the heatmap is the proportion of the maximum normalized count for a given gene per nuclear cycle

Movie 1. Representative *Slbp* embryo with full arrest in NC13
Slbp embryo has slower syncytial blastoderm nuclear cycles and ends the syncytial blastoderm cycles prematurely at NC13. It gastrulates one cell cycle early with about half the number of cells compared to WT. Still images from this movie are represented in Figure 1A. Scale bar represents 50 µm.

Movie 2. Representative *Slbp* embryo partially arrested in NC13
Slbp embryo has slower syncytial blastoderm nuclear cycles and partially arrests at NC13. It gastrulates normally with sections of the embryo in NC13 and NC14. Scale bar represents 50 µm.

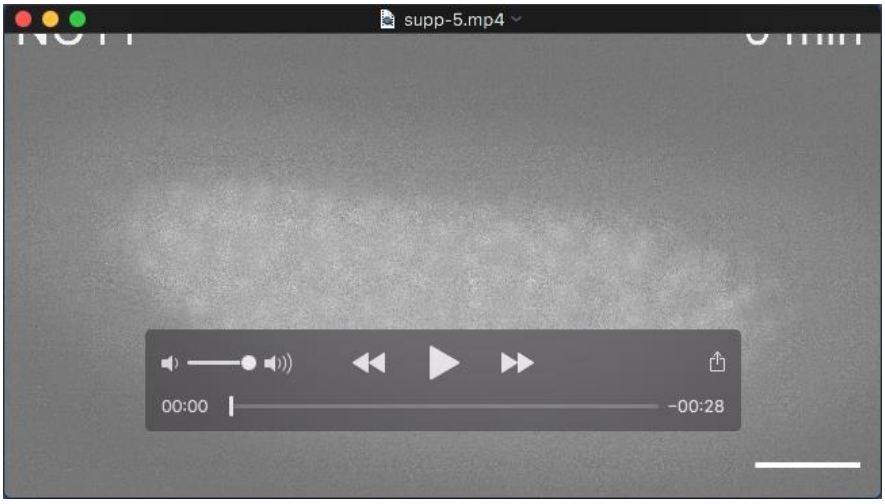

Movie 3. Representative *abo* embryo with extra division
abo embryo has a shortened nuclear cycle 14 and goes on to have a 15th and 16th nuclear cycle before attempting gastrulation. Scale bar represents 50 μm.

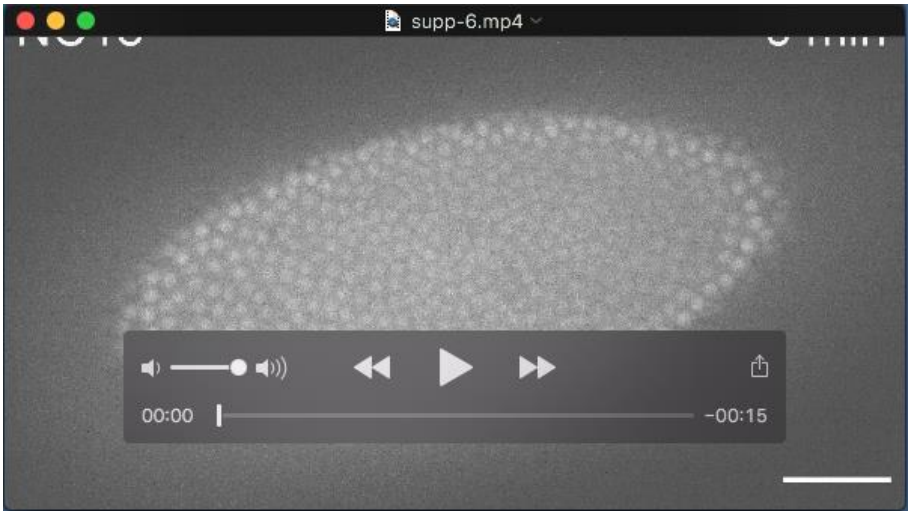

Movie 4. Representative *abo* embryo partially dividing into NC15
abo embryo has a normal NC14 before partially mitosing into NC15. It begins gastrulation while in the process of division and displays ectopic furrow formation. Scale bar represents 50 μm.

Table S1. Syncytial blastoderm phenotypes of histone depletion and overexpression
Range of phenotypes during the syncytial blastoderm stage from *Slbp* and *abo* embryos. The percent of occurrence is noted in the table and total number in parenthesis beside this value. “No nuclei” is defined as no nuclei make it to the embryo’s surface during the course of live imaging which generally occurs ~90 mins after egg laying. “Catastrophic fallout” is defined as fallout which prohibits the embryo from successfully reaching the onset of gastrulation. “NC13” is defined as embryos which initiate their long cell cycle pause at NC13 instead of at NC14. “NC13/14” is defined as embryos which initiated their long cell cycle pause with part of the embryo in NC13 and another in NC14. “NC14” is defined as embryos which go through the syncytial blastoderm stage normally and initiate their cell cycle pause at NC14. “NC14/15” is defined as embryos which undergo a partial extra division before the onset of gastrulation. “NC15” is defined as embryos which undergo a complete extra division before the onset of gastrulation. We excluded from all analysis the ~70% of *Slbp* embryos which have defective blastoderm formation as have been previously reported in *Slbp* mutants and nulls (Sullivan et al., 2001; Iampietro et al., 2014). As previously described the majority of *abo* embryos arrest before the syncytial blastoderm stage (Tomkiel et al., 1991; Tomkiel et al, 1995). We therefore excluded these and *abo* embryos which undergo catastrophic fallout from analysis. However, of the ~40% of embryos that form blastoderm, ~6% do a complete extra division and another ~4% do a partial extra division.

Click here to Download Table S1

Table S2: Differentially expressed gene counts for all genotypes and cell cycles
The number of genes in each category for all differential expression analysis conducted in this manuscript.

Click here to Download Table S2

Table S3: Differentially expressed genes in all *Slbp* to WT comparisons
Table with results from the differential gene expression analysis (using DESeq2) including FDR adjusted p-values that were used to provide significance thresholds for all *Slbp* comparisons.

Click here to Download Table S3

Table S4: Gene lists for differentially expressed genes in all Slbp comparisons
Gene names and identifiers for all genes identified as differentially expressed in *Slbp* at either timepoint.

Click here to Download Table S4

Table S5: Normalized gene counts for *Slbp* and WT at each timepoint
Table with the normalized gene counts for *Slbp* and WT for each timepoint. These values are plotted in Figure 2B and S3D.

Click here to Download Table S5

Table S6: Comparison of previous datasets to differentially expressed genes identified in this study
Number of genes and overlaps in each category of comparison between all differentially expressed genes identified in this study and the Lott et. al (2011), De Renzis et. al. (2007), and Lu et. al (2009) datasets (gene lists for previous datasets included as Table S22). P-values generated by a two-sided Fisher's exact test. These numbers underlie the overlaps displayed in Figures 2D, 3D, S3E, and S6.

Click here to Download Table S6

Table S7: Differentially expressed genes in *abo* NC14 to WT NC14 comparisons
Table with results from the differential gene expression analysis (using DESeq2) including FDR adjusted p-values that were used to provide significance thresholds for the pooled *abo* comparison.

Click here to Download Table S7

Table S8: Gene lists for differentially expressed genes in *abo* NC14 to WT NC14 comparisons
Gene names and identifiers for all genes identified as differentially expressed for the pooled *abo* datasets.

Click here to Download Table S8

Table S9: Normalized gene counts for *abo* and WT at NC14
Table with the normalized gene counts for *abo* and WT for pooled dataset. These values are plotted in Figures 3B.

Click here to Download Table S9

Table S10: Differentially expressed genes in *abo* timecourse comparisons
Table with results from the differential gene expression analysis (using DESeq2) including FDR adjusted p-values that were utilized to provide significance thresholds for the *abo* timecourse comparison.

Click here to Download Table S10

Table S11: Gene lists for differentially expressed genes in *abo* timecourse comparisons
Gene names and identifiers for all genes identified as differentially expressed in the timecourse *abo* datasets.

Click here to Download Table S11

Table S12: Normalized gene counts for *abo* timecourse
Table with the normalized gene counts for *abo* and WT timecourse dataset. These values are plotted in Figure S5C.

Click here to Download Table S12

Table S13: Transcriptional trajectory of all genes detected between Pre9 to NC14 for the wild-type
Classification of all genes into “transcription”, “flat”, and “degraded” derived from Pre9 vs NC14 comparison in WT as described in figure 4A and Methods.

Click here to Download Table S13

Table S14: Differentially expressed gene distribution compared to WT transcriptional trajectory
Counts from advance gene-category classification representing histone manipulations v/s wild-type differential expression at a given stage compared to the temporal transcriptional profile in wild-type for the same set of genes (see Table 13 and Methods for more details). These numbers are used in Figures 4B and S7.

Click here to Download Table S14

Table S15: Differentially expressed genelist for genes in *Slbp* compared to WT transcriptional trajectory
Gene names and identifiers for all genes identified as differentially expressed in *Slbp* and classified into “transcription”, “flat”, and “degraded” categories derived from Pre9 vs NC14 comparison in WT. The comparisons to WT NC14 are used as the *Slbp* gene list in Figure 4B.

Click here to Download Table S15

Table S16: Differentially expressed genelist for *abo* timecourse compared to WT transcriptional trajectory
Gene names and identifiers for all genes identified as differentially expressed in abo timecourse and classified into “transcription”, “flat”, and “degraded” categories derived from Pre9 vs NC14 comparison in WT. These genes lists are used as the *abo* gene lists in Figures 4B and S7.

Click here to Download Table S16

Table S17: Comparison of modENCODE data and DE genes from *Slbp*
Table with gene numbers, overlaps and Fisher's exact test results for promoter peaks from different embryonic modENCODE ChIP-seq factors quired for overlap with *Slbp* DE genes belonging to transcriptional categories defined as new transcription, flat, and degradation with appropriate background. These enrichments are plotted in Figue 4B.

Click here to Download Table S17

Table S18: Comparison of modENCODE data and DE genes from *abo* timecourse
Table with gene numbers, overlaps and Fisher's exact test results for promoter peaks from different embryonic modENCODE ChIP-seq factors quired for overlap with *abo* DE genes belonging to transcriptional categories defined as new transcription, unchanged and degradation with appropriate background. These enrichments are plotted in Figure 4B.

Click here to Download Table S18

Table S19: Effects of thresholds cutoffs on result reproducibility
Table detailing the number of genes in each set for all comparisons with different combinations of p-value and expression fold change cutoffs. Note the marked loss of genes in the WT NC13 to WT NC14 comparison when expression cutoffs are applied.

Click here to Download Table S19

Table S20: Differentially expressed genes are also expressed in WT
Table showing the percent of genes in each comparison that were detected at all in the stage matched WT controls. The vast majority of genes in all comparisons are present in WT, just in different abundance indicating that our results are not the result of genome wide dysregulation.

Click here to Download Table S20

Table S21: Raw and mapped read counts
Table showing the number of raw reads and mapped reads for all datasets generated in this study.

Click here to Download Table S21

Table S22: Gene lists from literature datasets used in this study
Gene lists from Lott et. al (2011), De Renzis et. al (2007), and Lu et. al (2009) used for comparisons in this study. These gene lists underlie the overlaps displayed in Figures 2D, 3D, S3E, and S6.

Click here to Download Table S22

Supplementary Materials and Methods:

RNA collection - single embryo and pooled

Single WT and *Slbp* embryos:
Collections for RNA from single embryos were dechorionated with 4% sodium hypochlorite, washed with DI water, and then mounted in Nunc microwell trays with water (VWR, 470378). Nuclear stage was observed via RFP fluorescence with microscopy settings previously described. Nuclear stage was determined by tracking embryo development as nuclei first surface at nuclear cycle 10. Individual *Slbp* and WT embryos were confirmed to be in the desired nuclear cycle interphase or mitosis. Minimal fallout criteria were established to avoid massive downregulation of zygotic transition observed in *Slbp* mutant and null embryos due to embryonic death (Sullivan et al., 2001; Iampietro et al., 2014; Lefebvre et al., 2017). Embryos that displayed groups of nuclei falling out of the blastoderm surface during the nuclear divisions before collection were discarded. Individual embryos were placed into an RNase free tube, lysed with a sterile needle. Then 100 µl of lysis buffer (Applied Biosystems, KIT0214) was added, and embryos were flash-frozen in liquid nitrogen, and stored at -80°C. Six biological replicates were collected for WT 13 and WT 14. Five biological replicates were collected for *Slbp* NC13.

Individual Pre-NC9 WT and *Slbp* embryos were collected after one-hour laying, confirmed to be preblastoderm stage by visualization in halocarbon oil (Sigma, H8773), and processed as above. Five biological replicates were collected for each genotype.

Single, time course WT and *abo* embryos:
For individual *abo* and WT embryos, each embryo was mounted as described above and observed at the beginning of NC10. We discarded any embryo whose cell cycle times deviated from our standard times by more than 1 minute in any cycle before collection. These stringent conditions mean that we eliminated any *abo* embryo that would have undergone an extra division and that changes in cell cycle times cannot explain differences in gene expression. Individual embryos were placed into an RNase free tube, lysed with a sterile needle. Then 100 µl of lysis buffer (Applied Biosystems, KIT0214) was added, and embryos were flash-frozen in liquid nitrogen, then stored at -80°C. Individual unfertilized WT and *abo* embryos were collected after one-hour laying and processed as above. Three biological replicates were collected for each genotype at each time point.

Pooled WT and *abo* embryos:
Collections for RNA from pooled WT and *abo* embryos were placed under halocarbon oil to determine developmental stage. Embryos between 5 and 15 minutes into nuclear cycle 14 were washed with DI water, dechorionated with 4% sodium hypochlorite, and washed with DI water again. Dechorionated embryos were placed in 100 ul RNAlater (Invitrogen, AM7020) and stored at 4°C. Embryos continued to develop for an additional ~15 minutes in RNAlater that resulted in their final collection time of 15-30 minutes into NC14. When 43, 45, and 45 embryos were collected per genotype for each respective replicate RNALater was removed and 100 ul of lysis buffer was added (Applied Biosystems, KIT02014. Embryos were lysed with a RNase free pestle, flash-frozen in liquid nitrogen, and stored at -80°C. RNA from all single and pooled embryos was isolated using PicoPure RNA Isolation Kit following the manufacturer's protocol (Applied Biosystems, KIT02014).

Quantification and Statistical Analysis

Data pre-processing
We split the barcodes using fastq-multx (1.3.1; Aronesty, 2013) and then utilized TrimGalore (0.5.0) using the default options to trim adapters. Trimmed reads were then quantified with Salmon (0.10.2; Patro et al., 2017) using the default options and the *Drosophila melanogaster* reference transcriptome (r6.19) obtained from flybase. The reference transcriptome was indexed using Salmon (0.10.2; Patro et al., 2017) with the default parameters prior to quantification (Table S21, S5, S9, S12).

Differential gene expression (DE) analysis
The counts generated by Salmon were utilized in DESeq2 (1.20.0; Love et al., 2014) to perform differential gene expression (DE) analysis comparing the "mutants" (*abo* or *Slbp*) to the wild-type per cell cycle. We used an FDR adjusted p-value cutoff $\leqslant 0.05$ to determine significantly DE genes and log2fold-change greater than or less than 0 to assign genes to the significantly differentially over- or under-expressed categories respectively. In cases where multiple sequencing runs were used, the technical replicates (i.e. same library run on different flow-cells), were almost identical as we did not detect any DE genes between these (Fig S3A and C, Fig S4A and C, Fig S5A and B). Thus, we collapsed the technical replicates by summing the read counts prior to DE analysis. We additionally imposed a minimal threshold of detecting at least 1 read in 2 or more samples, after collapsing the technical replicates and prior to performing the DE analysis. To visualize similarities between biological replicates of all samples we used the plotPCA function in DESeq2 to visualize the samples in 2D spanned by their first two principal components (Figures S3A, S4A and S5A). We also plotted the Spearman's rank correlation of the normalized counts as a heatmap to visualize correlations across all samples for a given experiment (Figures S3C, S4C and S5B). We did not detect a substantial difference in the total number of transcripts across different time points in a given experiment (Tables S5,S9,S12 and S21). However, due to degradation of maternal and accumulation of zygotic transcripts, not all transcripts are detected in all timepoints. To determine if the DE genes were maternal, zygotic, dependent on the N/C ratio or time dependent, we tested whether there was a significant overlap between the DE genes and relevant gene lists from literature via a two-sided Fisher's exact test (Table S22). An overlap with a p-value $\leqslant 0.05$ was considered as significant. To visualize the enrichment and de-enrichment of specific factors as a heatmap, we multiplied the log10 p-values by +1 for enrichment (shades of red) and -1 for de-enrichment for plotting (shades of blue) based on the magnitude of the odds ratio (>1 or <1 respectively) in Figures 2D, 3D, S3E and S5. See table S6 for all comparisons.

Advance gene-category classification
To generate a robust set of differentially expressed genes across multiple cell cycles we utilized Fisher's p-value combination method implemented in the metaRNASeq R package (1.0.2; Rau et al., 2014), to combine the p-values from all of the independent tests between the mutant and wild-type per cell cycle and generated a global FDR adjusted p-value for each gene across all cell cycles. We then assigned a gene significantly DE if it had a global FDR adjusted p-value $\leqslant$ 0.05. Subsequently, we inferred the signs of the p-value combined DE genes by comparing with differentially up or down-regulated genes identified at each cell cycle (Table S3, S7, and S10). We excluded any gene that was identified as significantly DE in the global analysis but were not identified as DE in any of the individual cell cycle. We further excluded all genes DE in the unfertilized embryo comparison from the larger set of DE genes, since these would reflect differences in maternal loading. To further classify whether DE genes were DE in mutants due

to excess transcription or degradation as compared to wild-type across time, we identified the genes that were upregulated, down-regulated or unchanged (flat) between NC14 and unfertilized embryo in only the wild-type, based on an FDR adjusted p-value $\leqslant$ 0.05 (Table S13). Any gene that is up-regulated in this window, we classify as "new transcription" and genes down-regulated as "degradation". These two categories largely meet expectations for gene membership. For instance, we find previously identified zygotic genes (De Renzis et al., 2007; Lott et al., 2011) over represented in the new transcription category. However, our classification is more permissive as transcripts that increase over time are included in the new transcription category regardless of the maternal contribution. We then determined how many of the DE genes (up/ down in mutant v/s wild-type) overlapped with the "new transcription" (trx), "degradation" (deg) and "flat" category of genes across time, as inferred from the wild-type data (Table S14, S15, and S16). Thus, genes that are differentially down-regulated in the mutant v/s wild-type comparison but overlap with "new transcription" category are those that have reduced transcription in the mutant over time as compared to the wild-type. While genes that are differentially up-regulated in the mutant v/s wild-type comparison but overlap with "degradation" category are those with increased stability in the mutant over time relative to the wild-type.

modENCODE comparisons

Chromatin signature identification using modENCODE ChIP-- data enrichment at promoters

To understand if genes belonging to the various DE gene-categories were enriched for other chromatin features, we performed an enrichment analysis using all modENCODE ChIP-seq and ChIP-chip datasets at developmental stages including 0-4h, 0-8h, 0-12h and 0-24h post-fertilization (modENCODE Consortium et al., 2009). While the 0-4h developmental stage provides the most appropriate comparison for our experiment, we wanted to make sure that our analysis captured all of the early embryogenesis related chromatin signatures. We converted the ChIP-peak coordinates to dm6 using a perl script provided by flybase for coordinate conversion and further re-annotated these peaks using ChIP-seeker R package (1.16.1; Yu et al., 2015), with TSS +/-500bp as being promoters. We subsequently extracted all the genes for which there is any ChIP-peak within the promoter region and performed a gene-set enrichment analysis with genes we identified from the relevant RNA-seq analysis. Enrichment analysis was performed via a two-sided Fisher's exact test in R with the appropriate gene categories. For example, we compared whether the genes that are underexpressed in a given histone manipulation v/s wild-type but are increasing over time in WT (i.e., *Slbp* or *abo* Under expressed and "new transcription" category as defined above) were enriched for the presence or absence of promoter peaks as compared to a background of all newly transcribed genes. An overlap with an FDR adjusted p-value $\leqslant$ 0.05 was considered as significant. To visualize the enrichment and de-enrichment of specific factors as a heatmap, we multiplied the log10 p-values by +1 for enrichment (shades of red) and -1 for de-enrichment for plotting (shades of blue) based on the magnitude of the odds ratio (>1 or <1 respectively) in Figure 4B. See supplemental tables S17 for *Slbp* and S18 for abo comparisons.

Supplementary References

Aronesty, E. (2013). Comparison of sequencing utility programs. *The Open Bioinformatics Journal* 7, 1-8. doi:10.2174/1875036201307010001

Iampietro, C., Bergalet, J., Wang, X., Cody, N. A. L., Chin, A., Lefebvre, F. A., Douziech, M., Krause, H. M. and Lécuyer, E. (2014). Developmentally Regulated Elimination of Damaged Nuclei Involves a Chk2-Dependent Mechanism of mRNA Nuclear Retention. *Dev. Cell* 29, 468-481. doi:10.1016/j.devcel.2014.03.025

Lefebvre, F. A., Benoit Bouvrette, L. P., Bergalet, J. and Lécuyer, E. (2017). Biochemical Fractionation of Time-Resolved Drosophila Embryos Reveals Similar Transcriptomic Alterations in Replication Checkpoint and Histone mRNA Processing Mutants. *J. Mol. Biol*. 429, 3264-3279. doi:10.1016/j.jmb.2017.01.022

Love, M. I., Huber, W. and Anders, S. (2014). Moderated estimation of fold change and dispersion for RNA-seq data with DESeq2. *Genome Biology* 15,

modENCODE Consortium, Celniker, S. E., Dillon, L. A. L., Gerstein, M. B., Gunsalus, K. C., Henikoff, S., Karpen, G. H., Kellis, M., Lai, E. C., Lieb, J. D., et al. (2009). Unlocking the secrets of the genome. *Nature* 459, 927-930. doi:10.1038/459927a

Patro, R., Duggal, G., Love, M. I., Irizarry, R. A. and Kingsford, C. (2017). Salmon provides fast and bias-aware quantification of transcript expression. *Nat. Methods* 14, 417-419. doi:10.1038/nmeth.4197

Rau, A., Marot, G. and Jaffrézic, F. (2014). Differential meta-analysis of RNA-seq data from multiple studies. *BMC Bioinformatics* 15, 91. doi:10.1186/1471-2105-15-91

Sullivan, E., Santiago, C., Parker, E. D., Dominski, Z., Yang, X., Lanzotti, D. J., Ingledue, T. C., Marzluff, W. F. and Duronio, R. J. (2001). Drosophila stem loop binding protein coordinates accumulation of mature histone mRNA with cell cycle progression. *Genes Dev*. 15, 173-187. doi:10.1101/gad.862801

Tomkiel, J., Pimpinelli, S. and Sandler, L. (1991). Rescue from the abnormal oocyte maternal-effect lethality by ABO heterochromatin in Drosophila melanogaster. *Genetics* 128, 583-594.

Tomkiel, J., Fanti, L., Berloco, M., Spinelli, L., Tamkun, J. W., Wakimoto, B. T. and Pimpinelli, S. (1995). Developmental genetical analysis and molecular cloning of the abnormal oocyte gene of Drosophila melanogaster. *Genetics* 140, 615-627.

Yu, G., Wang, L.-G. and He, Q.-Y. (2015). ChIPseeker: an R/Bioconductor package for ChIP peak annotation, comparison and visualization. *Bioinformatics* 31, 2382-2383. doi:10.1093/bioinformatics/btv145